ANALYSIS OF THE STABILITY DOMAIN OF PLANAR SYMPLECTIC MAPS USING INVARIANT MANIFOLDS

M. Giovannozzi

July 18, 1996

Abstract

In a previous paper we showed that, for the one-parameter area-preserving Hénon map, the domain in phase space where stable motion occurs can always be computed by using the invariant manifolds emanating from the hyperbolic fixed point of period one, regardless of the value of the parameter.

We present here a generalization of this result to a large class of symplectic polynomial mappings of the plane. Even in this case it is possible to show that the stability domain is given by the inner envelope of the invariant manifolds of a low period (one or two) hyperbolic fixed point.

Numerical simulations are presented. They were performed on different maps, including a model of relevance for accelerator physics.

1

1 Introduction

One of the main topics in the study of non-linear Hamiltonian systems is the determination of the region in phase space where bounded motion occurs. This problem has deep implications in various of science including accelerator physics. A hadron collider can be well described within the framework of Hamiltonian theory and the problem of the *dynamic aperture*, which is related to the region in phase space where stable motion occurs, is vital. To safely operate with the beam it is necessary that the stable region is big enough to accommodate the circulating particles with some safety margin. This imposes tight constraints on the design of a circular machine and it requires a good insight into the sources of instabilities.

For two-dimensional non-linear systems it is possible to define unambiguously an area in phase space where the motion is stable for arbitrarily long periods. In fact the phase space has a well-known structure [1, 2]: around the origin, which is usually chosen to be a stable fixed point, there are closed curves (1D KAM tori), and wherever the non-linear frequency satisfies a resonant condition the invariant curves are broken into islands. When non-linearities are dominant, one reaches a stability border beyond which a fast escape to infinity occurs. This stability border is what we have called the dynamic aperture. In this case the KAM tori separate different phase space domains, i.e. an initial condition inside a KAM torus cannot cross it: therefore, there exists a last connected invariant curve whose interior represents a set of stable initial conditions. Outside this curve, there can only be islands of stability, scattered in the sea of initial conditions which escape to infinity.

In a higher dimension the situation is completely different: the KAM tori do not separate different domains of phase space; therefore the concept of last invariant curve, surrounding stable initial conditions, is no longer valid [1, 2]. This implies that initial conditions arbitrarily close to the origin can slowly move away from it by a process similar to diffusive motion. Hence, strictly speaking, only the origin is stable for arbitrary times. This phenomenon due to the intrinsic topology of the phase space is universally known as *Arnold Diffusion* [3].

The standard approach to determine the stable region is to follow the evolution of a set of initial conditions distributed in the phase space. Their stability can be determined by checking whether they stay bounded, i.e. within a given distance from the origin, over a given time. This technique has the main drawback of giving little theoretical insight into the causes for

the instabilities and, furthermore, it is very CPU time consuming.

In previous papers we presented an analytical method [4, 5, 6] to determine the stable region in phase space of a simple planar Hamiltonian map. This approach allows the determination of the stability border of the Hénon map [7] following the invariant manifolds that emanate from the hyperbolic fixed point of the map. The key point of this method is that, although the Hénon map is actually a one-parameter family of maps, the result holds true regardless of the value of the parameter. The topology of the phase space depends critically on the value of the parameter; however, it is always possible to reconstruct exactly the stable region of this system from knowledge of the hyperbolic fixed point of period one.

In the present paper we generalize this result to a large class of planar area-preserving maps, namely maps which can be decomposed into involutions. Through a careful analysis of the existence and stability of the fixed points of such maps, we will show that the stability domain, i.e. the region in phase space of stable motion, is always given by the inner envelope of the invariant manifolds emanating from a fixed point of low period (one or two).

Furthermore we will present the results of numerical simulations carried out on a model representing a two-dimensional version of a circular accelerator, the CERN Super Proton Synchrotron, showing that the method is even more general and can be applied to realistic planar systems.

The structure of the paper is as follows: Section 2 discusses the problem of computing the fixed points for a symplectic map which can be decomposed into *involutions* (also called *reversible maps*). Section 3 reports some results on the existence of hyperbolic fixed points. In Section 4 we define the invariant manifolds and explain how to construct them numerically. The results of the numerical simulations on a simple model with a cubic non-linearity are presented in Section 5. In Section 6 some numerical experiments performed on a realistic model are described. Finally, some concluding remarks are made in Section 7.

2 Fixed points of reversible maps

In this section we will present some important results [8, 9, 10, 11] concerning the fixed points of a special class of symplectic maps.

A map $\mathbf{F}$ of $\mathbb{R}^{2n}$ which is symplectic, i.e. its Jacobian determinant is unity,

is called *reversible* if it is the product of two *involutions*, namely

$$\mathbf{F} = \mathcal{I}_1 \circ \mathcal{I}_2 \quad \mathcal{I}_1^2 = \mathcal{I}_2^2 = I, \tag{1}$$

where I is the identity matrix in $\mathbb{R}^{2n}$. This peculiar factorization imposes tight constraints on the existence and location of the fixed points and can be exploited to simplify the problem of their computation.

We recall that a point $\mathbf{x}$ is called a *fixed point* of $\mathbf{F}$ if it satisfies the equation

$$\mathbf{F}(\mathbf{x}) = \mathbf{x}. \tag{2}$$

Similarly, fixed points of order m, or m cycles, can be defined as the fixed points of the mth iterate of the map

$$\mathbf{F}^{\circ m}(\mathbf{x}) = \mathbf{x}, \tag{3}$$

where

$$\mathbf{F}^{\circ m}(\mathbf{x}) = \underbrace{\mathbf{F}(\mathbf{F}(\mathbf{F}(\cdots \mathbf{F}(\mathbf{x})\cdots)))}_{m \text{ times}}. \tag{4}$$

The first result one can prove is the following.

Theorem 1. *Given a symplectic map* $\mathbf{F}$ *of* $\mathbb{R}^{2p}$ *such that* $\mathbf{F} = \mathcal{I}_1 \circ \mathcal{I}_2$ *with* $\mathcal{I}_1, \mathcal{I}_2$ *two involutions, if* $\mathbf{x}$ *is a point of* $\mathbb{R}^{2p}$ *satisfying*

$$\begin{cases} \mathcal{I}_1(\mathbf{x}) & = & \mathbf{x} \\ \\ \mathcal{I}_2\left(\mathbf{F}^{\circ n}(\mathbf{x})\right) & = & \mathbf{F}^{\circ n}(\mathbf{x}) \end{cases} \tag{5}$$

then $\mathbf{F}^{\circ 2n+1}(\mathbf{x}) = \mathbf{x}$.

Similarly, if $\mathbf{x}$ *is a solution of one of the two systems*

$$\begin{cases} \mathcal{I}_1(\mathbf{x}) & = & \mathbf{x} \\ \\ \mathcal{I}_1\left(\mathbf{F}^{\circ n}(\mathbf{x})\right) & = & \mathbf{F}^{\circ n}(\mathbf{x}) \end{cases} \tag{6}$$

$$\begin{cases} \mathcal{I}_2(\mathbf{x}) & = & \mathbf{x} \\ \\ \mathcal{I}_2\left(\mathbf{F}^{\circ n}(\mathbf{x})\right) & = & \mathbf{F}^{\circ n}(\mathbf{x}) \end{cases} \tag{7}$$

then $\mathbf{F}^{\circ 2n}(\mathbf{x}) = \mathbf{x}$.

3

Proof. We will show the validity of the first result only, as the second one can be proved in the same way.

As a first step it is worthwhile noting that from the factorization in Eq. (1) follows

$$\mathcal{I}_1 \circ \mathbf{F}^{\circ m} = \mathcal{I}_2 \circ \mathbf{F}^{\circ m-1}, \quad \mathbf{F}^{\circ m} \circ \mathcal{I}_2 = \mathbf{F}^{\circ m-1} \circ \mathcal{I}_1; \tag{8}$$

and using the properties of the involutions combined with Eq. (5), one obtains that

$$
\begin{aligned}
\mathbf{F}^{\circ 2n+1}(\mathbf{x}) &= \mathbf{F}^{\circ n+1} \circ \mathbf{F}^{\circ n}(\mathbf{x}) = \mathbf{F}^{\circ n+1} \circ \mathcal{I}_2 \circ \mathbf{F}^{\circ n}(\mathbf{x}) \\[2mm]
&= \mathbf{F}^{\circ n} \circ \mathcal{I}_1 \circ \mathbf{F}^{\circ n}(\mathbf{x}) = \mathbf{F}^{\circ n} \circ \mathcal{I}_2 \circ \mathbf{F}^{\circ n-1}(\mathbf{x}) \\[2mm]
&= \mathcal{I}_1(\mathbf{x})
\end{aligned}
\tag{9}
$$

The last relation follows by applying Eq. (8) repeatedly, thus proving the theorem.

We will now consider a less general case of planar symplectic maps. We will choose the two involutions such that $\mathcal{I}_1$ will be a linear transformation of $\mathbb{R}^2$, and $\mathcal{I}_2$ a non-linear transformation of the plane. For the first transformation it is possible to write down the explicit expression. In fact, if we neglect the trivial possibility that $\mathcal{I}_1$ coincides with the identity matrix, the general form of a linear involution of $\mathbb{R}^2$ is given by

$$\mathcal{I}_1: \quad \begin{pmatrix} x' \\ y' \end{pmatrix} = \begin{pmatrix} \alpha & \beta \\ \dfrac{1-\alpha^2}{\beta} & -\alpha \end{pmatrix} \begin{pmatrix} x \\ y \end{pmatrix}, \tag{10}$$

where α, β are free parameters. It is a remarkable property of this transformation that it represents a reflection about the straight line of the equation

$$y = \frac{1-\alpha}{\beta} x. \tag{11}$$

Obviously such a line represents the locus of fixed points of $\mathcal{I}_1$.

As far as the non-linear transformation is concerned, we impose the following form:

$$\mathcal{I}_2: \begin{pmatrix} x' \\ y' \end{pmatrix} = \begin{pmatrix} 1 & 0 \\ 0 & -1 \end{pmatrix} \begin{pmatrix} x \\ y + P_n(x) \end{pmatrix}, \tag{12}$$

4

where $P_n(x) = \sum_{j=2}^{n} p_j x^j$ is a polynomial of degree n in the x variable only. The locus of the fixed points of the transformation shown in Eq. (12) can be easily determined:

$$y = -\frac{P_n(x)}{2}. \tag{13}$$

Again it can be shown that locally the transformation $\mathcal{I}_2$ represents a reflection about the curve of Eq. (13). In the following we will use the notation $\mathcal{F}ix\,(\mathcal{I}_l)$ for the set of fixed points of $\mathcal{I}_l$. The reason for the choice of the two particular transformations $\mathcal{I}_1, \mathcal{I}_2$ will be discussed in detail later. By using these assumptions it is possible to strengthen the results stated in Theorem 1. In fact it is possible to show the following.

Theorem 2. *Let* **F** *be a planar symplectic map factorized into involutions* $\mathcal{I}_1, \mathcal{I}_2$ *of types shown in Eqs. (10) and (12), respectively. Then* **x** *is a fixed point of* **F** *iff it satisfies*

$$\begin{cases} \mathcal{I}_1(\mathbf{x}) & = & \mathbf{x} \\[2mm] \mathcal{I}_2(\mathbf{x}) & = & \mathbf{x}\,. \end{cases} \tag{14}$$

Proof. We have already shown that the condition in Eq. (14) is sufficient; however, it remains to be proven that it is also necessary. The relation expressing **x** as a fixed point of **F** reads

$$\begin{cases} (\alpha - 1)x - \beta y - \beta P_n(x) & = & 0 \\[3mm] \dfrac{1 - \alpha^2}{\beta}x + (\alpha - 1)y + \alpha P_n(x) & = & 0\,, \end{cases} \tag{15}$$

and after a little algebra we obtain

$$\begin{cases} y & = & \dfrac{\alpha - 1}{\beta}x - P_n(x) \\[3mm] \dfrac{\alpha - 1}{\beta}x & = & \tfrac{1}{2}P_n(x)\,. \end{cases} \tag{16}$$

It can be readily seen that Eq. (16) is equivalent to the condition $\mathbf{x} \in \mathcal{F}ix\,(\mathcal{I}_1) \bigcap \mathcal{F}ix\,(\mathcal{I}_2)$.

The geometrical interpretation of the previous result is clear: the fixed points of period one are exactly the intersections of the loci of the fixed points

5

of the two transformations $\mathcal{I}_1, \mathcal{I}_2$ into which the map $\mathbf{F}$ is decomposed. A similar result holds even for the fixed points of $\mathbf{F}^{\circ 2}$.

Theorem 3. *Let $\mathbf{F}$ be a planar symplectic map factorized into involutions $\mathcal{I}_1, \mathcal{I}_2$ of the types in Eqs. (10) and (12), respectively. Then $\mathbf{x}$ is a fixed point of $\mathbf{F}^{\circ 2}$ iff it fulfils the following condition:*

$$\begin{cases} \mathcal{I}_2(\mathbf{x}) & = & \mathbf{x} \\ \\ \mathcal{I}_2\left(\mathbf{F}(\mathbf{x})\right) & = & \mathbf{F}(\mathbf{x}) \; . \end{cases} \tag{17}$$

Proof. We have already shown that if $\mathbf{x}$ satisfies Eq. (7) for $n = 1$ then it is a fixed point of $\mathbf{F}^{\circ 2}$. In addition we will show that with the new hypothesis on the form of the two involutions, if $\mathbf{x}$ is a solution of

$$\begin{cases} \mathcal{I}_1(\mathbf{x}) & = & \mathbf{x} \\ \\ \mathcal{I}_1\left(\mathbf{F}(\mathbf{x})\right) & = & \mathbf{F}(\mathbf{x}) \end{cases} \tag{18}$$

then $\mathbf{x}$ is a fixed point of $\mathbf{F}$ and therefore a trivial solution of $\mathbf{F}^{\circ 2}(\mathbf{x}) = \mathbf{x}$. By writing the equations and taking into account the expression of the two involutions, we obtain

$$\begin{cases} y & = & \dfrac{1 - \alpha}{\beta} x \\ \\ \dfrac{1 + \alpha - 2\alpha^2}{\beta} x + \alpha P_n(x) & = & \dfrac{(1 - \alpha)(2\alpha - 1)}{\beta} x - (1 - \alpha) P_n(x) \; . \end{cases} \tag{19}$$

It is apparent that the second equation is equivalent to

$$\frac{1 - \alpha}{\beta} x = -\frac{P_n(x)}{2} \; ,$$

hence $\mathbf{F}(\mathbf{x}) = \mathbf{x}$. As a consequence only the solutions of Eq. (7) for $n = 1$ are non-trivial roots of $\mathbf{F}^{\circ 2}$.

It remains to be proven that the condition is also necessary. This can easily be seen by writing the equation $\mathbf{F}^{\circ 2}(\mathbf{x}) = (\mathbf{x})$ in the equivalent form $\mathbf{F}(\mathbf{x}) = \mathbf{F}^{-1}(\mathbf{x})$. Therefore

$$\begin{cases} \alpha x - \beta y - \beta P_n(x) & = & \alpha x + \beta y \\ \\ \dfrac{1 - \alpha^2}{\beta} x + \alpha y + \alpha P_n(x) & = & -\dfrac{1 - \alpha^2}{\beta} x + \alpha y - P_n(\alpha x + \beta y) \; , \end{cases} \tag{20}$$

6

and from this we obtain

$$
\begin{cases}
y & = & -\frac{1}{2}P_n(x) \\[2ex]
\dfrac{1-\alpha^2}{\beta}x + \dfrac{\alpha}{2}P_n(x) & = & -\frac{1}{2}P_n(\alpha x - \frac{\beta}{2}P_n(x)) \ .
\end{cases}
\tag{21}
$$

It is clear that Eq. (21) coincides with Eq. (17).

Some insight can be gained by interpreting the previous result from a geometrical point of view. The meaning of condition (17) is the following: if the initial point $\mathbf{x}$ belongs to the locus $\mathcal{F}ix\,(\mathcal{I}_2)$ and, furthermore, if its image under the map $\mathbf{F}$ is also a point in $\mathcal{F}ix\,(\mathcal{I}_2)$, then $\mathbf{x}$ is a fixed point of period two. The action of the map on a point of $\mathcal{F}ix\,(\mathcal{I}_2)$ is simply a reflection about the fixed line of $\mathcal{I}_1$. Therefore, for a fixed point of period two to exist the set $\mathcal{F}ix\,(\mathcal{I}_2)$ must contain at least one point together with its reflection about the fixed line of $\mathcal{I}_1$. One can apply this result to see that this condition is never fulfilled for the quadratic Hénon map, thus explaining why it does not have any real fixed point of period two (see [7]).

2.1 Planar maps and physical models

In the previous section we showed how the existence of a fixed point is linked to the decomposition of a map into two involutions. From the general class of transformations which fulfil the involutive condition we selected a subset. Now we would like to justify this choice by examining the link between such transformations and physical models.
In many mathematical physics problems one is interested in the study of systems governed by a Hamiltonian $\mathcal{H} = \mathcal{H}(q,p;t)$ of the type

$$
\mathcal{H}(x,p;t) = \frac{p^2}{2} + \frac{\omega^2}{2}x^2 + G(x)\sum_{n=-\infty}^{+\infty}\delta(t-nT),
\tag{22}
$$

where $G(x) = \sum_{k=3}^{\infty}g_k x^k$. This system represents a non-linear oscillator. The equations of motion can be readily integrated thanks to the presence of the periodic δ function. Therefore, one obtains the following map:

$$
\mathbf{H}(\omega): \quad \begin{pmatrix} x' \\ y' \end{pmatrix} = \begin{pmatrix} \cos \omega T & -\sin \omega T \\ \sin \omega T & \cos \omega T \end{pmatrix} \begin{pmatrix} x \\ y + \dfrac{g(x)}{\omega} \end{pmatrix},
\tag{23}
$$

7

where [in Eq. (23)] we have used

$$g(x) = -\frac{dG(x)}{dx}, \qquad y = \frac{p}{\omega}. \tag{24}$$

In the mathematical literature $\mathbf{H}$ is called the *Poincaré section* of the Hamiltonian $\mathcal{H}(x, p; t)$.

It can be shown that under the assumption that $G(x)$ is a polynomial function of finite order, $\mathcal{H}$ represents a fundamental object in accelerator physics, namely a FODO cell containing a non-linear element in the thin lens approximation [2] expressed in normalized Courant–Snyder coordinates [12]. The rotation matrix in Eq. (23) accounts for the linear elements of the cell, while $g(x)$ is the contribution of the non-linear element. Therefore, if one is interested in applications to accelerator physics the proper object to study is

$$\mathbf{H}_n(\omega) : \quad \begin{pmatrix} x' \\ y' \end{pmatrix} = \begin{pmatrix} \cos \omega & -\sin \omega \\ \sin \omega & \cos \omega \end{pmatrix} \begin{pmatrix} x \\ y + P_n(x) \end{pmatrix}, \tag{25}$$

with $P_n(x) = \sum_{j=2}^n p_j x^j$, $T = 1$ and $\omega \in [0, 2\pi]$. In practice it is possible to restrict the interval of variation of the ω to $[0, \pi]$: for $\omega > \pi$ it suffices to consider $\omega - \pi$ and to change the sign of the odd terms in the polynomial $P_n(x)$. In the accelerator physics literature, the map $\mathbf{H}_n(\omega)$ is called a *one-turn map* or *transfer map*.

Furthermore it can immediately be seen that $\mathbf{H}_n(\omega)$ can be decomposed into two involutions

$$\mathcal{I}_1 : \quad \begin{pmatrix} x' \\ y' \end{pmatrix} = \begin{pmatrix} \cos \omega & \sin \omega \\ \sin \omega & -\cos \omega \end{pmatrix} \begin{pmatrix} x \\ y \end{pmatrix}, \tag{26}$$

and

$$\mathcal{I}_2 : \quad \begin{pmatrix} x' \\ y' \end{pmatrix} = \begin{pmatrix} 1 & 0 \\ 0 & -1 \end{pmatrix} \begin{pmatrix} x \\ y + P_n(x) \end{pmatrix}. \tag{27}$$

These involutions are exactly the same as those used in the previous section with

$$\alpha = \cos \omega \qquad \beta = \sin \omega. \tag{28}$$

This particular form of $\mathcal{I}_1$ permits a stable fixed point at the origin (which is always the case for physical situations).

8

3 Existence and stability of low-period fixed points

The results proved in the previous section concerning the calculation of fixed points can be combined to prove the following

Theorem 4. *Let $\mathbf{H}_n(\omega)$ be a planar symplectic map of the type*

$$H_n(\omega) : \begin{pmatrix} x \\ y \end{pmatrix} = R(\omega) \begin{pmatrix} x \\ y + P_n(x) \end{pmatrix} \quad \omega \in [0, \pi], \tag{29}$$

where $P_n(x) = \sum_{j=2}^{n} p_j x^j$. Then,

(i) *If $n = 2l$, at least one fixed point of period one exists other than the origin for all values of $\omega \in [0, \pi]$.*

(ii) *If $n = 2l + 1$ and $p_{2l+1} < 0$, at least one fixed point of period one exists other than the origin for all values of $\omega \in [0, \pi]$.*

(iii) *If $n = 2l + 1$ and $p_{2l+1} > 0$, at least two fixed points of period two exist other than the origin for all the values of $\omega \in [0, \pi]$.*

Proof.

(i) For the proof it is sufficient to consider the geometrical meaning of Eq. (14).

(ii) As for (i).

(iii) In this case it should be clear that the existence of fixed points of period one cannot be guaranteed for arbitrary values of ω. To prove this statement we will make use of Eq. (17). It can be shown that this condition is equivalent to

$$2x \sin \omega + P_{2l+1}(x) \cos \omega + P_{2l+1}\left(x \cos \omega - \frac{\sin \omega}{2} P_{2l+1}(x)\right) = 0 . \tag{30}$$

To eliminate the trivial solutions given by the fixed points of period one, which satisfy

$$2x \tan \frac{\omega}{2} + P_{2l+1}(x) = 0, \tag{31}$$

9

we will consider

$$
\mathcal{F}(x) = \frac{2x \sin \omega + P_{2l+1}(x) \cos \omega + P_{2n+1}\left(x \cos \omega - \frac{\sin \omega}{2} P_{2n+1}(x)\right)}{2x \tan \frac{\omega}{2} + P_{2l+1}(x)} .
$$
(32)

Therefore, the equation $\mathcal{F}(x) = 0$ will allow the non-trivial fixed points of period two to be calculated.

It can immediately be seen that

$$
\mathcal{F}(0) = \frac{2}{1 + \tan^2 \frac{\omega}{2}} > 0 \quad \forall \quad \omega \in [0, \pi].
$$
(33)

Furthermore, it is possible to show that the asymptotic behaviour of $\mathcal{F}$ for $x \to \pm\infty$ is given by

$$
\mathcal{F}(x) \approx \frac{-p_{2n+1}^{2n+2} [\sin \omega]^{2l+1} x^{(2n+1)^2} \left[1 + \mathcal{O}(\frac{1}{x})\right]}{p_{2n+1} x^{2n+1} \left[1 + \mathcal{O}(\frac{1}{x})\right]}
$$

$$
\approx -p_{2n+1}^{2n+1} [\sin \omega]^{2l+1} x^{2n(2n+1)} \left[1 + \mathcal{O}\left(\frac{1}{x}\right)\right] .
$$

Therefore the sign of the limit depends only upon the sign of p_{2l+1}: if it is positive then $\mathcal{F}(x) \to -\infty$, which, combined with the property in Eq. (33), proves that at least two solutions of $\mathcal{F}(x) = 0$ are always present for all values of $\omega \in [0, \pi]$.

Now we will consider the problem of the stability of the fixed points determined so far. The first step is to consider how they can be classified. Close to the fixed point $\mathbf{x}$ the motion is determined by the linear part of the generic map $\mathbf{F}$, i.e. the Jacobian matrix $\mathbf{F}_L$

$$
\begin{pmatrix} \Delta x' \\ \Delta y' \end{pmatrix} = \begin{pmatrix} \dfrac{\partial F_1}{\partial x} & \dfrac{\partial F_1}{\partial y} \\ \dfrac{\partial F_2}{\partial x} & \dfrac{\partial F_2}{\partial y} \end{pmatrix} \begin{pmatrix} \Delta x \\ \Delta y \end{pmatrix} + \text{higher orders,}
$$
(34)

where F_1 and F_2 are the two components of $\mathbf{F}$. Therefore the stability of the fixed point is determined by the eigenvalues (λ_1, λ_2) of $\mathbf{F}_L$. Owing to the

area-preserving property they must satisfy the condition $\lambda_1\lambda_2 = 1$ so that only three situations are allowed:

$$
\begin{array}{llll}
\lambda_1, \lambda_2 \in \mathbf{C} & \lambda_1 = \lambda_2^* & \text{elliptic case} \\
\lambda_1, \lambda_2 \in \mathbb{R} & \lambda_1 \neq \lambda_2 & \text{hyperbolic case} & (35) \\
\lambda_1, \lambda_2 \in \mathbb{R} & \lambda_1 = \lambda_2 = 1 & \text{parabolic case.}
\end{array}
$$

In the following we will make use of the concept of *Poincaré index of a map*. Given a closed curve $\mathcal{C}$ which does not pass through any fixed point of a map $\mathbf{F}$, the index of $\mathcal{C}$, $Ind_{\mathcal{C}}$, is defined as the number of times the vector

$$
\mathbf{v}(\mathbf{x}) = \mathbf{F}(\mathbf{x}) - \mathbf{x} \quad \mathbf{x} \in \mathcal{C} \tag{36}
$$

circles the origin as the point $\mathbf{x}$ moves along $\mathcal{C}$.

It is clear that $Ind_{\mathcal{C}}$ is a function with integer values. Moreover, some properties of such a function are readily deduced

- $Ind_{\mathcal{C}}$ depends continuously on the curve $\mathcal{C}$. Furthermore, when the map $\mathbf{F}$ is dependent on certain parameters, the index depends smoothly on the same parameters.

- A curve enclosing only one fixed point will have an index equal to $-1, +1, +1$ according to the classification of the fixed point: hyperbolic, elliptic or hyperbolic with inversion, respectively.

- The index of a curve enclosing different fixed points is the sum of the indexes of each fixed point.

- The index of a closed orbit of $\mathbf{F}$ is $+1$.

We will now return to the specific maps $\mathbf{H}_n(\omega)$. Let us indicate with $x_i, i = 1, \ldots k$ the k solutions of the polynomial equation

$$
P_n(x) = 0. \tag{37}
$$

It is clear that $(x_i, 0)$ are fixed points of $\mathbf{H}_n(0)$. Furthermore, we define

$$
\begin{aligned}
x_{\max} &= \max_{i=1,\ldots k} x_i \\
x_{\min} &= \min_{i=1,\ldots k} x_i \ .
\end{aligned}
$$

For $\omega \neq 0$ the fixed points $(x_{\max}, 0)$ and $(x_{\min}, 0)$ will move along a branch of the curve $\mathcal{F}ix\,(\mathcal{I}_2)$ according to the intersection with the line $\mathcal{F}ix\,(\mathcal{I}_1)$.

11

In this general case we will use the notation $x_{\max}(\omega)$, $x_{\min}(\omega)$ to take into account both the dependence on ω and on the initial points $x_{\max}$, $x_{\min}$. Using these concepts it is possible to prove the following.

Theorem 5. *Given a map $\mathbf{H}_n(\omega)$ decomposed into two involutions $\mathcal{I}_1(\omega), \mathcal{I}_2$ of the types shown in Eqs. (26) and (27), the following holds:*

(i) *If $n = 2l$ and $p_{2l} > 0$, the point*

$$\mathbf{x}_{\min}(\omega) = \left[x_{\min}(\omega), -\frac{P_{2l}(x_{\min}(\omega))}{2} \right] \tag{38}$$

is hyperbolic over the whole interval $\omega \in [0, \pi]$.

(ii) *If $n = 2l$ and $p_{2l} < 0$, the point*

$$\mathbf{x}_{\max}(\omega) = \left[x_{\max}(\omega), -\frac{P_{2l}(x_{\max}(\omega))}{2} \right] \tag{39}$$

is hyperbolic in the whole interval $\omega \in [0, \pi]$.

(iii) *If $n = 2l + 1$ and $p_{2l+1} < 0$, the points*

$$\mathbf{x}_{\min}(\omega) = \left[x_{\min}(\omega), -\frac{P_{2l+1}(x_{\min}(\omega))}{2} \right]$$

$$\mathbf{x}_{\max}(\omega) = \left[x_{\max}(\omega), -\frac{P_{2l+1}(x_{\max}(\omega))}{2} \right]$$

are hyperbolic over the whole interval $\omega \in [0, \pi]$.

Proof.

(i) It can be seen immediately that there exists a value ω_1 such that for $\omega \in [\omega_1, \pi]$ there will be only two fixed points of period one, namely the origin ($\mathbf{x}_{\mathrm{orig}}$) and $\mathbf{x}_{\min}(\omega)$. If we consider a closed curve $\mathcal{C}$ surrounding $\mathbf{x}_{\mathrm{orig}}$ and $\mathbf{x}_{\min}(\omega)$ then $Ind_{\mathcal{C}}$ is the sum of the indexes of the the two points. The origin is elliptic by definition, therefore it has an index of $+1$. Hence $\mathbf{x}_{\min}(\omega)$ must be hyperbolic, i.e. with an index of -1. Otherwise $Ind_{\mathcal{C}}$ would be equal to $+2$, but it can be shown that no continuous map can satisfy $Ind_{\mathcal{C}} = +2$ for any closed curve $\mathcal{C}$. Furthermore, $\mathbf{x}_{\min}(\omega)$ remains hyperbolic even for $\omega \in [0, \omega_1]$. In fact in this interval it moves along a monotonic branch of the curve $\mathcal{F}ix(\mathcal{I}_2)$ and no bifurcation can occur. Therefore its stability cannot change.

12

(ii) The same approach as for (i) can be used.

(iii) In this case it is always possible to find a value ω_1 such that only three distinct fixed points are present, namely the origin $\mathbf{x}_{\mathrm{orig}}$, $\mathbf{x}_{\max}(\omega)$ and $\mathbf{x}_{\min}(\omega)$. The origin is elliptic (index $+1$) by construction, therefore three possibilities are left for the stability of the other two fixed points, i.e. their indexes could be $+1$ and $+1$, $+1$ and -1, or -1 and -1, respectively. The first case is forbidden as it would give a global index of $+3$. The second is not allowed because two out of the three fixed points would give an index of $+2$. Hence only the last possibility is compatible with the properties of the index. Moreover, this result can be extended to the interval $[0, \omega_1]$ as no bifurcation occurs along the branches of the curve $\mathcal{F}ix\,(\mathcal{I}_2)$ swept by the fixed points. This proves the theorem.

A similar statement holds for the fixed points of period two.

Theorem 6. *Given a map* $\mathbf{H}_{2l+1}(\omega)$ *decomposed into two involutions* $\mathcal{I}_1(\omega), \mathcal{I}_2$ *of the types shown in Eqs. (26) and (27), such that* $p_{2l+1} > 0$, *there exist two fixed points of period two,* $\mathbf{x}_1(\omega) = (x_1(\omega), y_1(\omega))$ *and* $\mathbf{x}_2 = (x_2(\omega), y_2(\omega))$ *with* $x_1(\omega) < x_{\min}$ *and* $x_2(\omega) > x_{\max}$, *which are hyperbolic over the whole interval* $\omega \in [0, \pi]$.

Proof. By using Eq. (17) it is clear that there exists a value ω_1 such that for $\omega \in [0, \omega_1]$ only three fixed points of period two exist: the origin $\mathbf{x}_{\mathrm{orig}}$ and what we have called $\mathbf{x}_1$ and $\mathbf{x}_2$. It is easy to show that the map $\mathbf{H}_{2l+1}(\omega)$ transforms $\mathbf{x}_1$ into $\mathbf{x}_2$ and vice versa, therefore the two points will have the same stability. Furthermore, they must be hyperbolic as it is not possible to construct a continuous map with an index of $+2$. Again the reasoning can be extended to the whole interval $[0, \pi]$ as in previous cases.

4 Invariant manifolds of symplectic maps

In Sections 2 and 3 we discussed the problem of determining the fixed points of a planar map when it can be expressed as the product of two involutions, and we investigated the existence of low-period hyperbolic fixed points $\mathbf{x}_{\mathrm{hyp}}$. In the hyperbolic case the two eigenvalues define two linear sets in the plane, $\mathcal{W}_{\mathrm{L}}^{\mathrm{u}}(\mathbf{x}_{\mathrm{hyp}})$ and $\mathcal{W}_{\mathrm{L}}^{\mathrm{s}}(\mathbf{x}_{\mathrm{hyp}})$, along which the motion induced by the linearized

map has an expanding (superscript u for unstable) or a contracting (superscript s for stable) behaviour. The subscript L indicates that these objects are linked with the linear part of the map. The interesting fact is that we can extend these sets to the original non-linear map $\mathbf{F}$, i.e. it is possible to define two subspaces emanating from the unstable fixed point such that these sets, called $\mathcal{W}^{\mathrm{u}}(\mathbf{x}_{\mathrm{hyp}})$ and $\mathcal{W}^{\mathrm{s}}(\mathbf{x}_{\mathrm{hyp}})$, show the same expanding or contracting behaviour. Furthermore, it is possible to prove that these sets are actually manifolds and that the eigenvectors of $\mathbf{F}$ are tangential to the manifolds $\mathcal{W}^{\mathrm{u,s}}(\mathbf{x}_{\mathrm{hyp}})$ at the fixed point. It should be evident that these manifolds are invariant sets for the map, namely

$$\mathbf{F}(\mathcal{W}^{\mathrm{u,s}}(\mathbf{x}_{\mathrm{hyp}})) = \mathcal{W}^{\mathrm{u,s}}(\mathbf{x}_{\mathrm{hyp}}) \ . \tag{40}$$

It is clear that a similar definition can be given in the case of higher order hyperbolic fixed points. In this case, all the previous definitions and properties hold, provided that the map $\mathbf{F}$ is replaced by its mth iterate $\mathbf{F}^{\circ m}$.

From the very definition it follows that the invariant manifolds have at least one intersection which is the hyperbolic fixed point. An additional intersection, $\mathbf{x}_{\mathrm{hom}}$, is either *homoclinic* or *heteroclinic* depending on whether the two intersecting manifolds emanate from the same hyperbolic fixed point. Provided the two manifolds are transversal, i.e. non-tangential, at the point $\mathbf{x}_{\mathrm{hom}}$, it can be proven that there must be other intersections, and that the set of intersections is countable. The key point is the invariance of the two manifolds. Therefore, unless the two manifolds coincide completely, which occurs in the integrable case, they will oscillate around each other.

Due to the area-preserving character of the map, the area enclosed between two successive intersections has to remain constant. Furthermore, the period of the motion tends to infinity as it approaches the hyperbolic fixed point, thus forcing the distance between successive intersections to decrease exponentially, and leading to larger and larger oscillations close to the hyperbolic fixed point.

To construct the whole sets $\mathcal{W}^{\mathrm{u,s}}(\mathbf{x}_{\mathrm{hyp}})$, it is sufficient to iterate many times a set of initial conditions belonging to a small part of these manifolds in the vicinity of $\mathbf{x}_{\mathrm{hyp}}$. Moreover, it turns out that these initial conditions can be chosen on the eigenvalues of the linearized map provided their distance to the hyperbolic fixed point is sufficiently small.

The interest in studying invariant manifolds lies in their relation to the stability domain of planar symplectic-maps. The stability domain of a planar map is the set of initial conditions $\mathbf{x} = (x, y)$ such that $\mathbf{F}^{\circ n}(\mathbf{x})$ is bounded

for arbitrary values of n. In [4] it is shown that for the case of the Hénon map [7] the stability domain is given by the inner envelope of the invariant manifolds emanating from the hyperbolic fixed point of period one. In Fig. 1 an example of the stated result is shown: the grey area represents the stability domain and the invariant manifolds are superimposed. The homoclinic oscillations are clearly visible and the agreement between the inner part of the manifolds and the shaded area is impressive. It is worthwhile noting that although the linear frequency is closed to the 1/4 resonance, it is possible to reconstruct the fourfold symmetry imposed by the resonance structure simply by using the hyperbolic fixed point of period one.
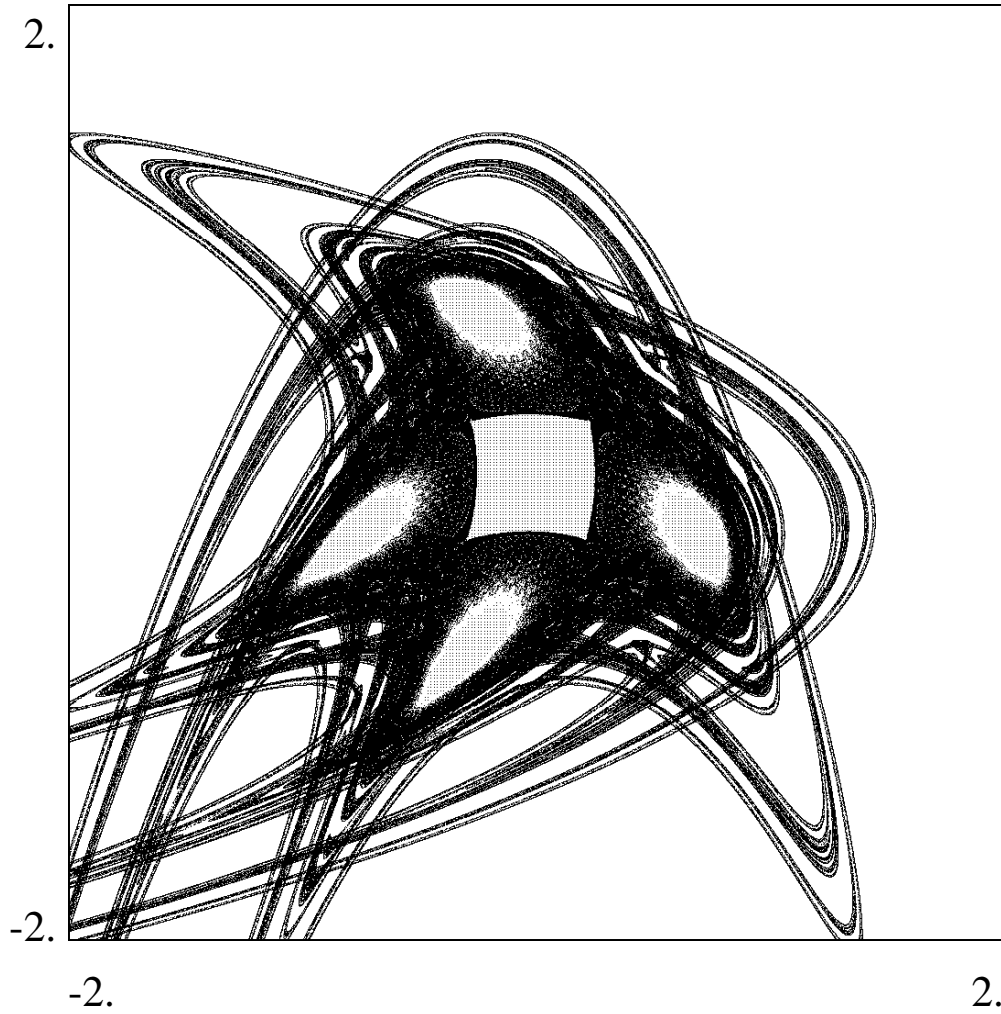
Figure 1: Invariant manifolds and stability domain for the Hénon map. The black area represents the stochastic layer where heteroclinic intersections between invariant manifolds emanating from hyperbolic fixed points of different order occur. The grey area represents the stability domain. The value of the linear frequency is $\omega/2\pi = 0.255$.

5 Stability results for the cubic map

In an attempt to generalize the result obtained for the Hénon map to other planar maps of the type $\mathbf{H}_n(\omega)$, we will study a map with cubic non-linearity, namely

$$H_3(\omega): \quad \begin{pmatrix} x' \\ y' \end{pmatrix} = R(\omega) \begin{pmatrix} x \\ y + p_2 x^2 + p_3 x^3 \end{pmatrix} , \tag{41}$$

using the results on the fixed points obtained previously. As already shown, such a map can be derived from the Hamiltonian [Eq. (22)] with

$$G(x) = -\omega \left(\frac{p_2}{3} x^3 + \frac{p_3}{4} x^4 \right) . \tag{42}$$

Obviously the coefficient of the quadratic term can be set to one by rescaling the variables. Moreover, the case where $p_2 = 1$ and p_3 is a free parameter has already been studied in [13]. Here then we will consider the simplified case $p_2 = 0$, thus allowing an analytical treatment of the problem without losing generality. Therefore, from now on, we will consider the following map

$$H_3(\omega): \quad \begin{pmatrix} x' \\ y' \end{pmatrix} = R(\omega) \begin{pmatrix} x \\ y + p_3 x^3 \end{pmatrix} , \quad p_3 \in \mathbb{R}, \quad \omega \in [0, \pi] . \tag{43}$$

Having set the quadratic term to zero, it is possible to rescale the variables such that $p_3 = \pm 1$. In fact, by defining new coordinates

$$X = \pm \sqrt{|p_3|} \qquad Y = \pm \sqrt{|p_3|} \tag{44}$$

the map (43) will read

$$\begin{pmatrix} X' \\ Y' \end{pmatrix} = R(\omega) \begin{pmatrix} X \\ Y + \mathrm{sgn}(p_3) X^3 \end{pmatrix} . \tag{45}$$

The first step will be to compute the fixed points of period one. By using Eq. (5),

$$\begin{cases} \text{if } p_3 > 0 \quad \text{then} \qquad \text{no real solution} \\ \text{if } p_3 < 0 \quad \text{then} \quad \mathbf{x}_{1,2} = \left(\pm \sqrt{\frac{2 \tan \frac{\omega}{2}}{|p_3|}}, \pm \sqrt{\frac{2 \tan^3 \frac{\omega}{2}}{|p_3|}} \right) . \end{cases} \tag{46}$$

As far as their stability is concerned, it is easily found that the trace of the linearization of $H_{3L}(\omega)$ is given by

$$\mathrm{Tr}\left[H_{3L}(\omega) \right] = 2 \frac{5 \tan^2 \frac{\omega}{2} + 1}{\tan^2 \frac{\omega}{2} + 1} , \tag{47}$$

17

and therefore the two fixed points are hyperbolic for all values of the linear frequency in the interval $[0, \pi]$. These results suggest that a straightforward generalization of the result obtained for the quadratic map to the cubic map is not possible. In fact, in the case where $p_3 > 0$ there are no real hyperbolic fixed points (in agreement with the results of the previous sections) and therefore no real invariant manifolds to be used in the determination of the stability domain of the map.

Hence we are forced to look for higher-order fixed points. The natural choice is to consider fixed points of order two. This task can be made considerably easier by applying the results of Section 2. It should be obvious that there are no real fixed points of period two in the case where $p_3 < 0$. Otherwise, for $p_3 > 0$ we have

$$\bar{\mathbf{x}}_{1,2} = \left(\pm\sqrt{\frac{2}{\tan\frac{\omega}{2}}}, \mp\sqrt{\frac{2}{\tan^3\frac{\omega}{2}}} \right) . \tag{48}$$

In this case too the stability can be easily determined, and it turns out that $\bar{\mathbf{x}}_{1,2}$ are hyperbolic for all values of $\omega \in [0, \pi]$.

With all these results to hand, we can perform the stability-domain analysis of the map [Eq. (45)]. The first point will be the study of the dynamics for the limit cases, namely $\omega = 0$ and $\omega = \pi$.

For $\omega = 0$, the map reduces to

$$\begin{cases} x' &= x \\ y' &= y + \mathrm{sgn}(p_3)x^3 \end{cases} \tag{49}$$

and this recurrence can easily be solved

$$\begin{cases} x_n &= x_0 \\ y_n &= y_0 + n\,\mathrm{sgn}(p_3)x_0^3 \ . \end{cases} \tag{50}$$

Therefore every initial condition is unstable as it tends to infinity under the iteration of the map.

For $\omega = \pi$, $R^2(\pi) = I$, therefore $\mathbf{H}_3(\pi)$ has the following expression

$$\begin{cases} x' &= -x \\ y' &= -y - \mathrm{sgn}(p_3)x^3 \ . \end{cases} \tag{51}$$

18

The general solution of the previous recurrence is

$$\begin{cases} x_n &=& (-1)^n x_0 \\[2mm] y_n &=& (-1)^n y_0 - (-1)^n n \, \mathrm{sgn}(p_3) x_0^3 \end{cases} \qquad (52)$$

and again we have instability for every initial condition.

In the general case of $\omega \neq 0$, the stability domain has to be analysed using the invariant manifolds, i.e. if $p_3 < 0$ one should use the hyperbolic fixed points of period one together with the related manifolds. Alternatively, if $p_3 > 0$ then the fixed points of period two should be used to compute the related invariant manifolds.

This fact has been checked by performing some numerical simulations. In Fig. 2 the results for $p_3 = -1$ are presented. The shaded area represents the stability domain, i.e. initial conditions which stay bounded under the iteration of the map. In the simulations, 10 000 iterates of the map have been used to check the stability of the initial conditions. The invariant manifolds emanating from the hyperbolic fixed points of period one are shown in the same plot. It is impressive that the invariant manifolds are able to reconstruct even the finest details of the stable region. This is due to the heteroclinic intersections: the invariant manifolds emanating from the fixed points of lowest period are connected to each other and to other manifolds through heteroclinic intersections. This mechanism allows the boundary of the stable area to be reached from outside.
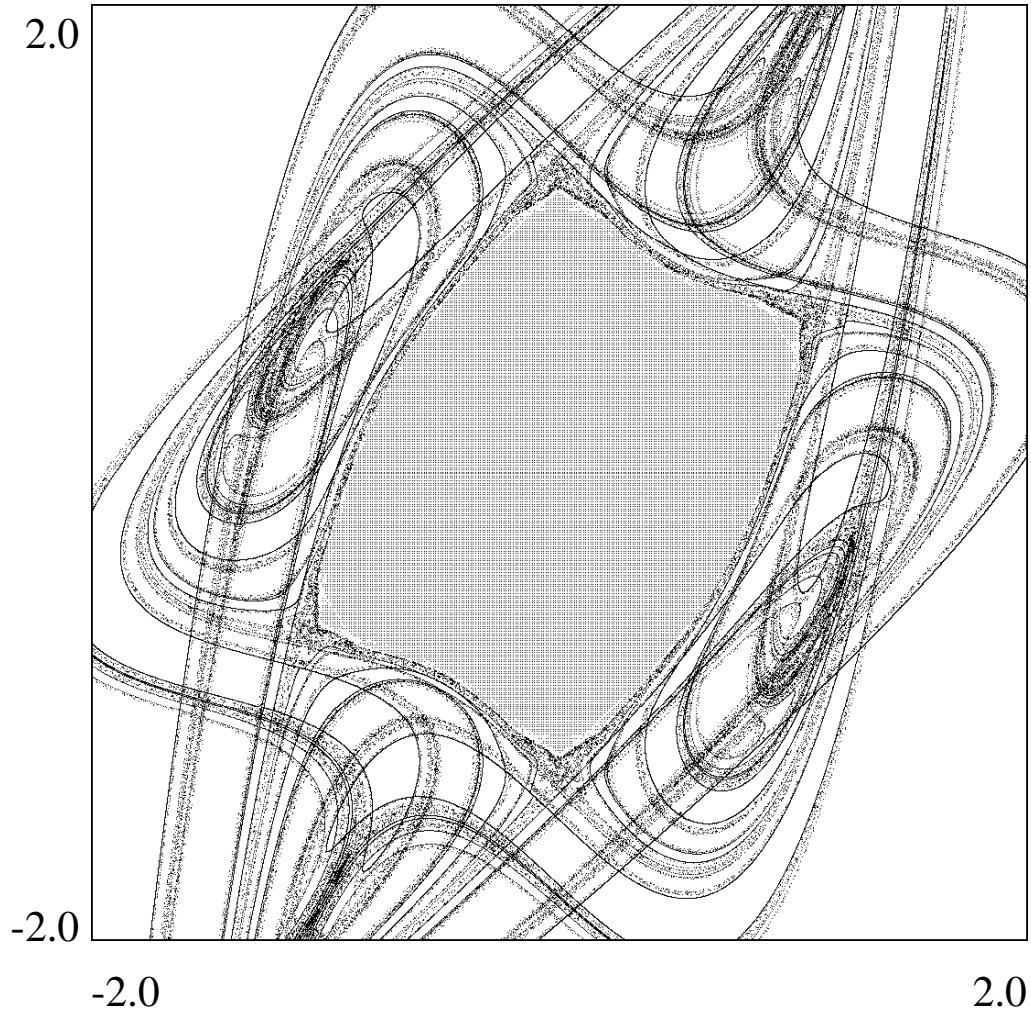
Figure 2: Invariant manifolds of the hyperbolic fixed points of period one and stability domain for the cubic map. The stability domain is represented by the grey area. The value of the linear frequency is $\omega/2\pi = 0.34$, while $p_3 = -1$.

To check that this result is truly general and that it does not depend on a specific value of ω, we have computed the stability domain as a function of the parameter ω for the case where $p_3 = -1$. In Fig. 3 the solid curve represents the minimum radius of the stability domain, i.e. the radius of the biggest disc embedded in the stable domain. Hence we take into account only the connected part of the stable area around the origin, disregarding

the stable islands which could possibly exist. The points shown in the same plot are computed using the invariant manifolds. More precisely they represent the minimum distance of the manifolds from the origin. Once again the agreement is impressive, thus reinforcing the result: the stability domain is given by the inner envelope of the invariant manifolds.

Finally we will consider the case where $p_3 = 1$ for a specific value of the linear frequency ($\omega = 0.255$). In Fig. 4 the stable area is shown (shaded region) together with the invariant manifolds emanating from the hyperbolic fixed points of period two. As in the previous examples, the agreement is excellent.
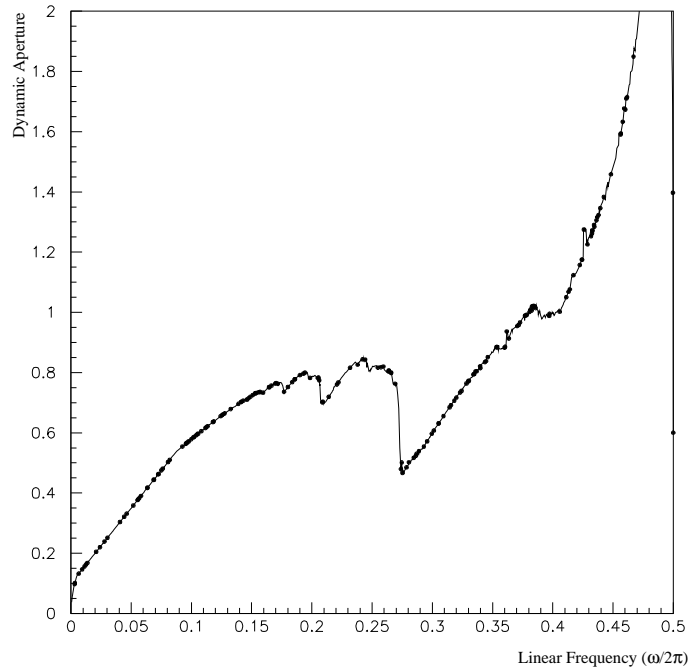
Figure 3: Stability domain as a function of the linear frequency for the cubic map ($p_3 = -1$). The solid line represents the minimum radius of the stability domain, computed by direct iteration of the map. The points represent the minimum distance from the origin of the invariant manifolds
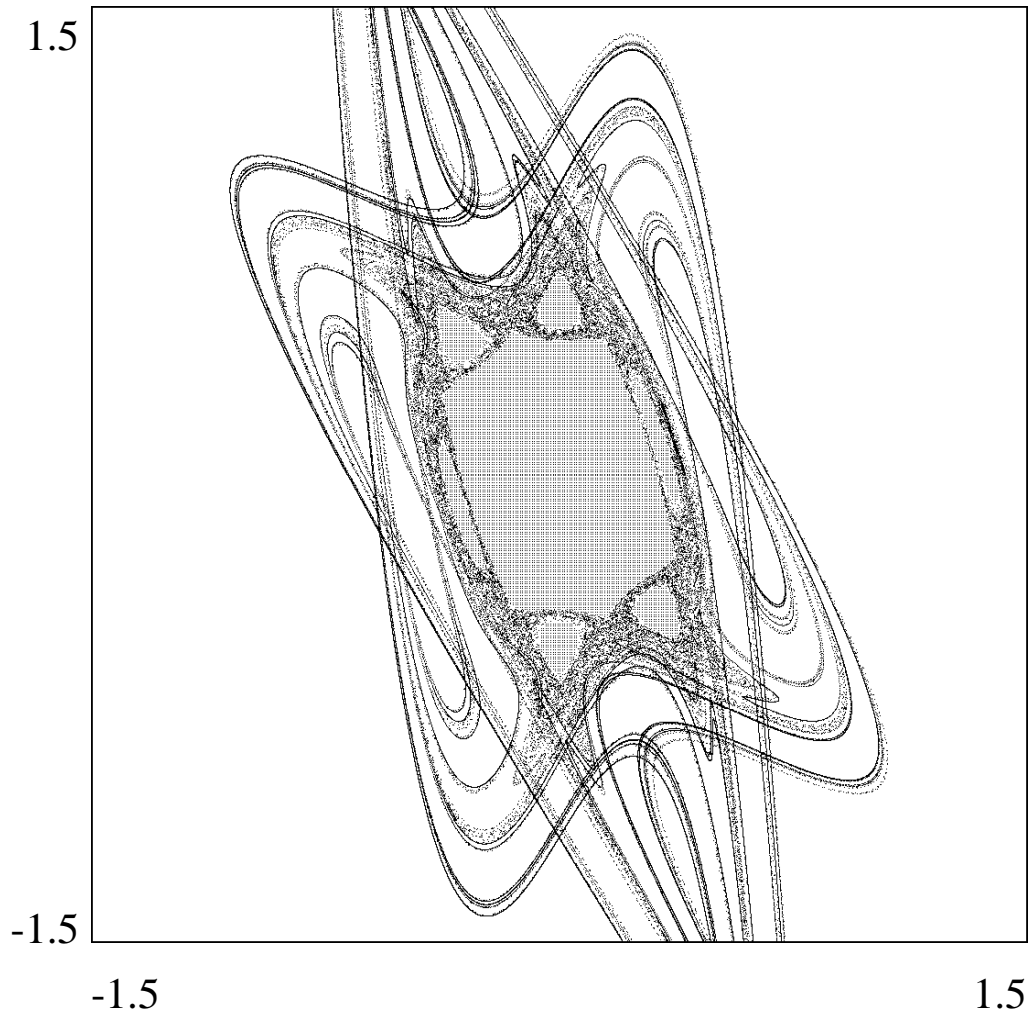
Figure 4: Invariant manifolds emanating from the hyperbolic fixed points of period two for the cubic map with linear frequency $\omega/2\pi = 0.255$ and $p_3 = 1$. The grey area is the stability domain as computed by direct iteration of the map.

At this point of our analysis, we can summarize the situation as follows:

- If $\mathbf{H}_n(\omega)$ is of even order, i.e. $n = 2k$, then real hyperbolic fixed points of period <u>one</u> exist for $\omega \in [0, \pi]$. These fixed points can be used to construct the invariant manifolds and to compute the stability domain as the inner envelope of such manifolds.

- If $\mathbf{H}_n(\omega)$ is of odd order, i.e. $n = 2k + 1$ and $p_{2k+1} < 0$, then again hyperbolic fixed points of period <u>one</u> exist for $\omega \in [0, \pi]$. This case can be treated in the same way as the one above.

- If $\mathbf{H}_n(\omega)$ is of odd order, i.e. $n = 2k + 1$ and $p_{2k+1} > 0$, then hyperbolic fixed points of period <u>two</u> exist. The invariant manifolds related to these fixed points determine the stability domain for $\omega \in [0, \pi]$.

6 A realistic model: the CERN SPS

To conclude this analysis we will present some results obtained for a more realistic model. We have applied the approach based on the invariant manifolds to a lattice representing a 2D version of the CERN Super Proton Synchrotron (SPS).

This machine has a symmetry of order six, with FODO cells of approximately 90 degrees phase advance. In addition to the linear elements, there is a certain number of non-linear magnets, namely sextupoles and octupoles. The sextupoles have a twofold function: to correct the chromatic effects produced by the quadrupoles (108 elements) and to extract the beam by exciting the third order resonance (8 elements). The octupoles are used to control the instabilities due to collective effects.

In the past years the SPS has been used to perform experiments of non-linear dynamics [14]. For these studies, the SPS is setup in a configuration where the eight extraction sextupoles are powered with currents ten times stronger than during normal operation, allowing the introduction of strong but controlled non-linearities. The octupoles are switched off.

In this configuration the real transfer map of the SPS can be approximated very accurately by composition of the eight transfer maps corresponding to the eight extraction sextupoles plus the linear elements in between, the chromatic sextupoles being neglected. Therefore the one-turn map can be written as

$$\mathbf{x}' = \mathbf{M}(\mathbf{x}) = \mathbf{M}_1 \circ \ldots \mathbf{M}_8(\mathbf{x}), \tag{53}$$

where $\mathbf{M}_j$ represents the transfer map of the jth extraction sextupole plus the linear elements up to the $(j + 1)$th sextupole. These maps have been computed using the program SIXTRACK [15]. The global map $\mathbf{M}$ has been transformed into normalized coordinates to deconvolve the rotation generated by the linear elements. The one-turn map then reads

$$\mathbf{y}' = \mathcal{M}(\mathbf{y}) = R(\omega) \circ \mathcal{N}(\mathbf{y}), \tag{54}$$

where $R(\omega)$ represents a rotation matrix, while $\mathcal{N}$ incorporates the non-linear part of the map. The linear frequency has been set to $\omega/2\pi = 0.636$, which coincides with the value normally used in the experiments.

To apply the approach used for maps of type $\mathbf{H}_n(\omega)$ it is necessary to determine the fixed points of the map [Eq. (54)]. The hyperbolic fixed points of the map $\mathcal{M}$ have been computed with the help of the program GIOTTO [16, 17, 18]. GIOTTO allows the phase space of a generic 2D map to be visualized and, at the same time, it has the capability to perform the computation of a certain number of dynamic indicators which are useful in the analysis of the map under consideration. For instance, it can compute the fixed points of arbitrary period using a bisection method [19]. As an example, we show in Fig. 5 the phase space of the map in Eq. (54). Some invariant curves are clearly visible together with a chain of islands of period five.

From the whole set of hyperbolic fixed points, the one which is furthest from the origin was chosen. Then the invariant manifolds were computed using the standard approach previously defined. The choice of the fixed point does not influence the result as the different manifolds are always connected (this is actually the key point of our method). In Fig. 6 we show the results. As usual, the grey area represents the stability domain as computed by direct iteration of the one-turn map of Eq. (54). The invariant manifolds are also superimposed on the same plot. As for the simple model of the cubic map studied in Section 5, we found excellent agreement between the stability domain and the inner envelope of the invariant manifolds. The stable islands in the large stochastic sea are perfectly reproduced, as is the border of the stable area, thus showing the generality of the method proposed here.
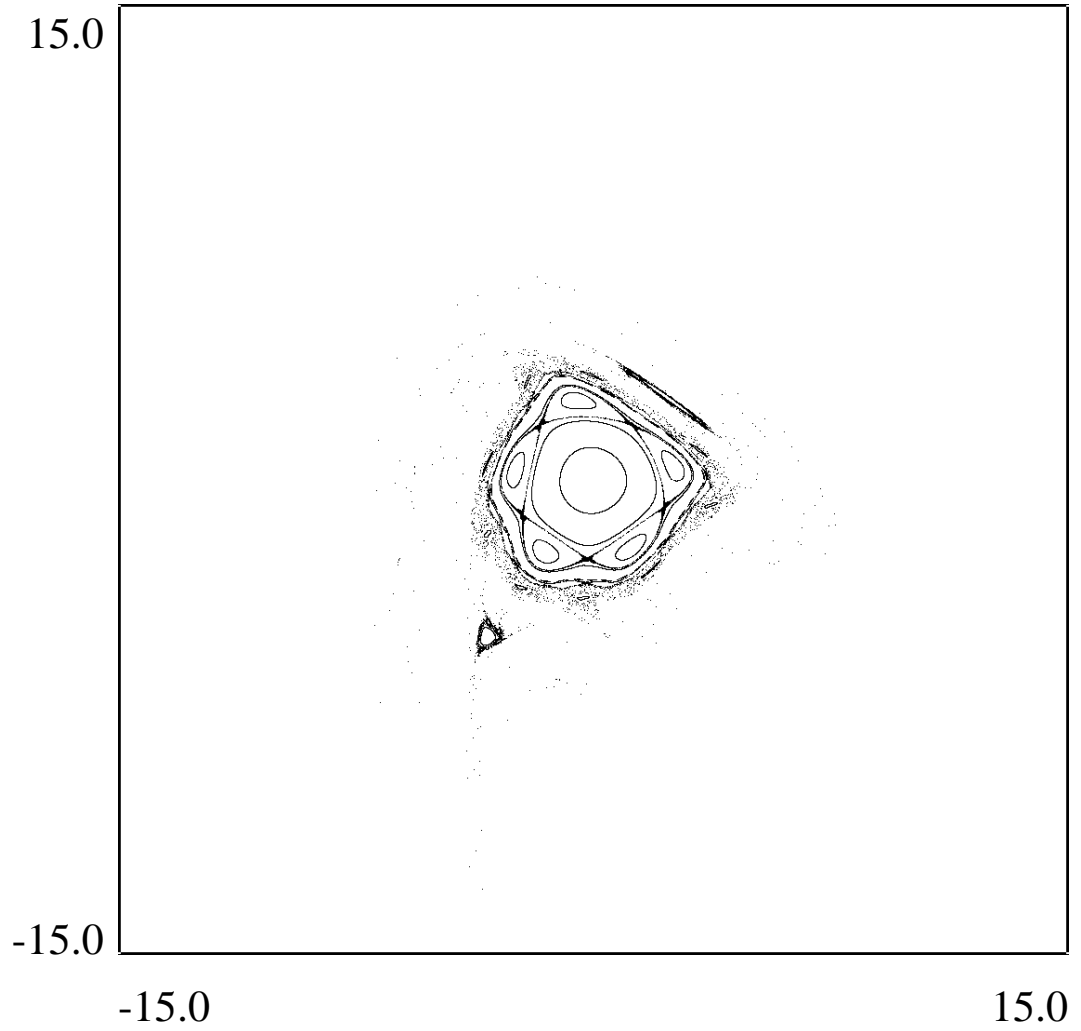
24

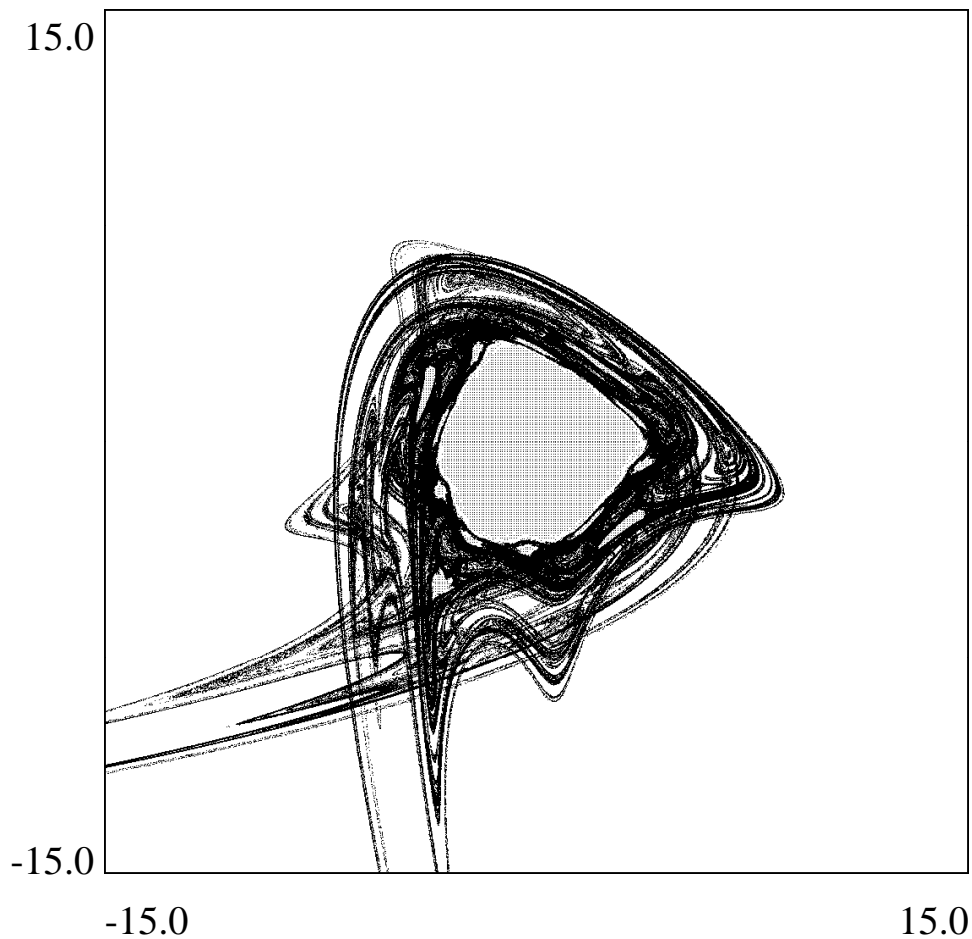Figure 5: Phase space portrait of the 2D model of the SPS lattice.

Figure 6: Invariant manifolds of the hyperbolic fixed point of period one for the 2D model of the SPS lattice. The grey area represents the stability domain as computed by direct iteration of the one-turn map.

7   Conclusions

In this paper we have presented the properties of the fixed points of a class of planar area-preserving maps which can be decomposed into involutions. This peculiarity allows the problem of finding the fixed points to be simplified and some results on the existence of hyperbolic fixed points of low period (one

or two) to be proved. Furthermore we have shown the connections between these maps and accelerators.

We have outlined how it is possible to use invariant manifolds to reconstruct the stability domain of a map decomposed into involutions, avoiding the direct iteration of a set of initial conditions, in order to test their stability. This approach is very powerful as it allows the stability domain in the whole interval of variation of the parameter ω to be determined using the same low-period hyperbolic fixed point.

Moreover, we have shown that the method is even more general, by presenting an application to a realistic model based on the lattice of the CERN Super Proton Synchrotron. In this case too the stability domain can be accurately reproduced using the invariant manifolds.

8 Acknowledgements

References

[1] J.D. Meiss, 'Symplectic maps, variational principles, and transport', Rev. Mod. Phys. **64** (1992) 795.

[2] A. Bazzani, G. Servizi, E. Todesco and G. Turchetti, 'Normal forms for symplectic maps and non-linear theory of betatronic motion', CERN 94–02 (1994).

[3] V.I. Arnol'd, 'Instability of dynamical systems with several degrees of freedom', Soviet Math. Dokl. **5** (1964) 581.

[4] M. Giovannozzi, 'Analysis of the stability domain for the Hénon map', Phys. Lett. **A182** (1993) 255.

[5] A. Bazzani, M. Giovannozzi, G. Servizi, E. Todesco and G. Turchetti, 'Computation of the dynamic aperture of a one dimensional model of a sextupole non-linearity, using analytical tools', Proc. Third European

Particle Accelerator Conference, ed. H. Henke et al. (Edition Frontières, Gif-sur-Yvette, 1992) 945.

[6] A. Bazzani, M. Giovannozzi, G. Servizi, E. Todesco and G. Turchetti, 'Resonant normal forms, interpolating Hamiltonians and stability analysis of area preserving maps', Physica **D64** (1993) 66.

[7] M. Hénon, 'Numerical study of quadratic area-preserving mappings', Q. Appl. Math. **27** (1969) 291.

[8] R. De Vogelaere, 'On the structure of symmetric periodic solutions of conservative systems with applications', *in* Contributions to the theory of non-linear oscillations, ed. S. Lefschetz (Princeton University Press, Princeton, 1958), Vol. IV, p. 53.

[9] J.M. Finn, 'Integrals of canonical transformations and normal forms for mirror machines Hamiltonian', PhD thesis, University of Maryland (1974).

[10] M. Giovannozzi, 'Analisi di stabilità per mappe Hamiltoniane e loro applicazioni alla fisica degli acceleratori' , Master thesis, University of Bologna (1989).

[11] M. Giovannozzi, 'Aspetti di dinamica non lineare con applicazioni in dinamica dei fasci', PhD thesis, University of Bologna (1993).

[12] E. Courant and H. Snyder, 'Theory of the alternating-gradient synchrotron', Annals of Physics **3** (1958) 1.

[13] M. Giovannozzi, 'Invariant manifolds and stability: some results for 1-D maps', AIP Conf. Proc. **292** (Particle and Fields) (1993) 385.

[14] W. Fischer, M. Giovannozzi and F. Schmidt, 'The dynamic aperture experiment at the SPS' CERN–SL/95–96 (1995) (AP) submitted to Phys. Rev. E.

[15] F. Schmidt, 'SIXTRACK: Single particle tracking code treating transverse motion with synchrotron oscillations in a symplectic manner', CERN–SL/91–52 (1990) (AP).

[16] T. Bountis, G. Servizi, G. Turchetti and M.N. Vrahatis, 'A procedure to compute the fixed points and visualize the orbits of a 2D map', CERN–SL/93–06 (1993) (AP).

[17] A. Bazzani, D. Bortolotti, M. Giovannozzi, G. Servizi, E. Todesco and G. Turchetti, 'GIOTTO: an interactive program for the analysis of 2D area preserving mappings', Proc. Fourth European Particle Accelerator Conference, ed. V. Suller et al. (Edition Frontières, Gif-sur-Yvette, 1994) 923.

[18] D. Bortolotti, M. Giovannozzi, G. Servizi, E. Todesco and M.N. Vrahatis, "GIOTTO: a code for the non-linear analysis of area-preserving mappings', Int. J. Mod. Phys. **C6** (1995) 651.

[19] M.N. Vrahatis, 'CHABIS: a mathematical software package for locating and evaluating roots of systems of non-linear equations', ACM Trans. Math. Softw. **14** (1988) 330.